Surface EMG for the Assessment of the Gait Performance in Hemiplegic Patients

Ivan Topalović, Suzana Dedijer Dujović, Ljubica Konstantinović and Dejan B. Popović, *Member, IEEE*

***Abstract*— We developed a method for assessment of the gait regularity in hemiplegic patients. We used a fully wearable system comprising ground reaction force sensors and inertial measurement units to record the dynamics and array electrodes and multichannel amplifiers for electromyography (EMG) mapping of activity of *tibialis anterior m*. during the gait. The fuzzy logic was applied to ground reaction force signals for estimating the gait symmetry. This paper introduces a new parameter for estimation of symmetry of muscle activities in the ipsilateral and contralateral legs based on the entropy of EMG maps. The presented method forms a set of gait parameters for quantifying the regularity of the patient's gait. The set of parameters are of interest for the assessment of the efficacy of the therapy.**

***Index Terms*—gait, EMG, EMG maps, IMU, wearable technology, drop foot**

I. Introduction

Cerebrovascular lesion in most cases leads partial paralysis of one side of the body (hemiplegia). Hemiplegia comprises an irregular posture, unevenly distributed support on legs when standing, slow and asymmetrical gait, rapid onset of fatigue, etc. [1].

The motor status of a hemiplegic patient can be assessed by the analysis of the gait regularity. There are a several scales for gait assessment: Rivermead Visual Gait Assessment (RVGA), Salford Gait Tool (SGT), Observational Gait Scale (OGS), Clinical Gait and Balance Scale (GABS), etc. [2]. The listed clinical scales are largely based on the visual observations made by the clinician.

Technological progress led to the reproducible and examiner independent methods for gait quantification. Different types of instrumentation are in use: sensor platforms for measuring the reaction forces of the ground and cameras with reflective markers for recording movement [3], inertial measurement units (IMU), and insoles for shoes with force sensors [4], walking paths with sensors [5], etc. These systems provide various information about gait mechanics: joints angles, angular velocities, ground reaction forces, etc. [6]. Electrophysiological signals (e.g., electromyography – EMG) carry important information about the motor systems responsible for the gait [7]. The combination of physiological signals and gait mechanics gives the possibility of qualitative and quantitative gait analysis, which includes the analysis of the movement actuators and its mechanics.

We presented a method for gait assessment based on temporal parameters [8, 9]. To obtain these parameters (gait cycle, step cycle, swing phase, stance phase, double support phase, and cadence) we used shoe insoles with built-in pressure sensors and IMUs to analyze gait mechanics and determine the characteristic moments that represent the boundary between individual gait phases. We showed in another study [10] the upgraded method where the EMG mapping was included. We have shown that there are significant differences between the intensities of EMG in specific regions on the paretic and nonparetic leg. We showed the presence of symmetrical shapes in EMG maps of ipsilateral and contralateral extremities and lack of intensity in the paretic side relative to nonparetic [11, 12]. As EMG maps represent digital images, in [13] we have shown the implementation of digital image processing techniques for analysis of EMG maps.

In this paper we presented the method for gait assessment based on temporal gait parameters and EMG mapping. The method quantifies the gait symmetry in electrical activities of muscle *tibialis anterior* (TA) in legs during the gait of hemiplegic patients. The TA muscle is responsible for lifting the toes. The lack of activity of the TA results with the drop foot and the gait starts to be abnormal since the toes are catching the ground during the swing phase of the gait cycle. We used the recordings of mechanical and EMG signals from the gait of a group of hemiplegic patients before and after standard medical treatment in the rehabilitation.

II. The Method

A. Instrumentation

To record monopolar EMG signals from the TA on both legs we used two custom designed circular 24-pad electrodes (d = 8 mm). Pads were fixed in 6 rows with different number of pads (5 pads in 1st and 2nd row, 4pads in 3rd and 4th row, and 3 pads in 5th and 6th row). Arrays were made of SA9327 EKG/EMG Ag-AgCl commercially available electrodes (Thought Technology Ltd., Montreal, QC, CA). All pads were

Ivan Topalović is with Institute of Technical Sciences of SASA, Knez Mihailova 35, 11000 Belgrade, Serbia (e-mail: topalovic_ivan@yahoo.com)

Suzana Dedijer Dujović is with the Clinic for rehabilitation "Dr Miroslav Zotović", Sokobanjska 13, 11000 Belgrade (e-mail: suzanadedijer@yahoo.com)

Ljubica Konstanitinović is with the Medical Faculty, University of Belgrade and Clinic for rehabilitation "Dr Miroslav Zotović", Sokobanjska 13, 1100 Belgrade (e-mail: ljubicakonstantinovic@yahoo.com)

Dejan B. Popović is with the School of Electrical Engineering, University of Belgrade, 73 Bulevar kralja Aleksandra, 11020 Belgrade, Serbia and Serbian Academy of Sciences and Arts (e-mail: dbp@etf.rs).

covered with AG936 conductivity gel (Axelgaard Manufacturing Co. Ltd., Lystrup, DK). We used disposable pre-gelled EMG Ag/AgCl electrodes with 10 mm flat pellets, Covidien BRD H124SG (Covidien, Medtronic, Dublin, IR) as ground and reference electrode.

Array electrodes were connected to two wearable 24-channel amplifiers Smarting® (https://mbraintrain.com/). The Smarting was designed for monopolar recordings of the cortical activities (brain-computer interface – BCI). Due to Bluetooth connection with PC Smarting has sampling rate limit at 500 Hz per channel. This limitation does not satisfy Nyquist criterion for EMG signals, but we validated the applicability of the Smarting® for estimation of EMG envelopes by comparing the recordings with the signals acquired by a professional EMG amplifier BioVision (BioVision, Wehrheim, DE) [14]. For recordings, we used the proprietary software of the Smarting®. Each Smarting system was connected to a separate PC.

For the recording of the gait mechanics we used instrumented insoles (Gait Teacher, https://rehabshop.rs/). Each insole comprises five pressure sensors and one IMU to record accelerations and angular velocities in all three directions. Insoles have wireless connection with PC. For the signal acquisition, we used the proprietary software of the Gait Teacher. In this study we used signals from the pressure sensors that are highly correlated with the ground reaction forces.

All three recording systems (two PCs with smarting systems and one PC connected to insoles system) were synchronized by Lab Stream Layer platform, which collects data from available streams from PCs connected in the same Local Area Network.

B. Subject and Procedure

One hemiplegic patient (female, 72-years, 175 cm, 71 kg, right side hemiplegia, uses four-legged cane) participated in our key study. She signed the informed consent approved by the ethics committee of the Clinic for rehabilitation "Dr Miroslav Zotović"). The whole procedure was supervised by a physiatrist.

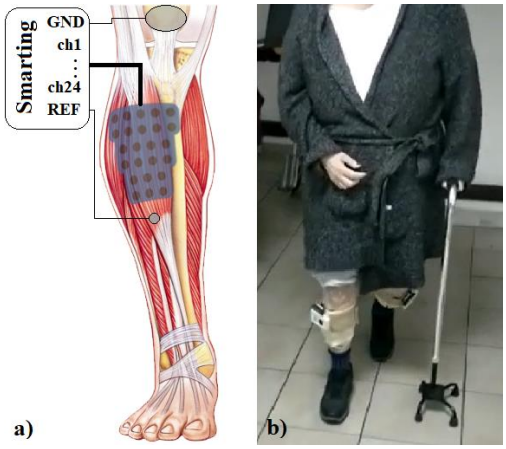

Fig. 1. a) Schematics of the electrode placement: array electrode was covering the region over TA muscle; ground electrode was placed over bony part of knee and the reference electrode was placed under the array along the longitudinal axis; b) Patient with experimental setup.

The array electrodes were placed symmetrically on both legs, covering the TA regions. Longer edge of the electrode was placed along the tibia, top of the electrode at 20 mm from the tibial tuberosity (Fig. 1). Ground electrodes were placed over *patella*, and reference electrodes were placed under the array electrodes, 10 mm along the longitudinal axis.

Subject's task was to walk in a straight line to cover the distance of 10 m. Before the recording subject was asked to stand with evenly distributed weight on both legs (as much as it was possible). Subject was asked to start and stop the gait on an auditory signal. The subject was asked to walk with the gait rate that she felt comfortable. The procedure was repeated three times in one session before and after three weeks of the therapy.

C. Data Processing

An original software in Matlab R2015a (MathWorks, Inc., Natick, MA, US) was used for processing.

We applied fuzzy logic on signals from pressure sensors to estimate the heel contact (HC; beginning of the stance phase) and toes off (TO; beginning of swing phase) moments. Detailed explanation can be found in [8, 9]. We estimated the following parameters: gait cycle (GC) – time between the two consecutive HC of the same leg; step cycle (SC) – time between the HC of the ipsilateral leg and the HC of the contralateral leg; stance phase (STP)– time between the HC and the TO of one leg; swing phase (SWP)– time between TO and HC of one leg; double support phase (DSP) – time when both legs are contacting the ground; gait cadence (GCD)– number of steps per unit time.

We applied high pass Butterworth filter (2nd order, cutoff frequency at 30 Hz) to EMG signals to stabilize the baseline and notch Butterworth filter (3rd order) at 50 Hz to minimize the impact of noise coming from the power lines. To remove the artefacts incurred during a heel strike we used FastICA method [15]. Recorded signals $\boldsymbol{x}$ (surface EMG) with artifacts can be represented as:

$$\boldsymbol{x} = \boldsymbol{A}\boldsymbol{s}; \tag{1}$$

$$\boldsymbol{x} = \begin{bmatrix} x_1 \\ \vdots \\ x_n \end{bmatrix}; \boldsymbol{s} = \begin{bmatrix} s_1 \\ \vdots \\ s_n \end{bmatrix}; \boldsymbol{A} = \begin{bmatrix} a_{11} & \cdots & a_{1n} \\ \vdots & \ddots & \vdots \\ a_{n1} & \cdots & a_{nn} \end{bmatrix};$$

where $\boldsymbol{s}$ are original activities of particular sources and $\boldsymbol{A}$ is the mixing matrix (matrix of constants).

Using the ICA algorithm, the weight factors $\boldsymbol{W}$ are calculated such that the separated components $\boldsymbol{u}$ are maximally statistically independent:

$$\boldsymbol{u}(t) = \boldsymbol{W}\boldsymbol{x}(t) = \boldsymbol{W}\boldsymbol{A}\boldsymbol{s}(t) \tag{2}$$

Fig. 2 shows the decomposition of 24 EMG signals from one array electrode (only one channel is shown on the top panel due to limited space) to 24 independent components (maximum number of components). Among the obtained components $\boldsymbol{u}$ (middle panel) the components with artifacts

stand out (examples are marked with red circles).We detected components that mostly contain artifacts, using visual inspection, and removed them manually, equating them with zero. After the components are deleted, the inversion reconstructs the EMG signals based on the remaining components:

$$\boldsymbol{x}(t) = \boldsymbol{W}^{-1}\boldsymbol{u}(t) \tag{3}$$

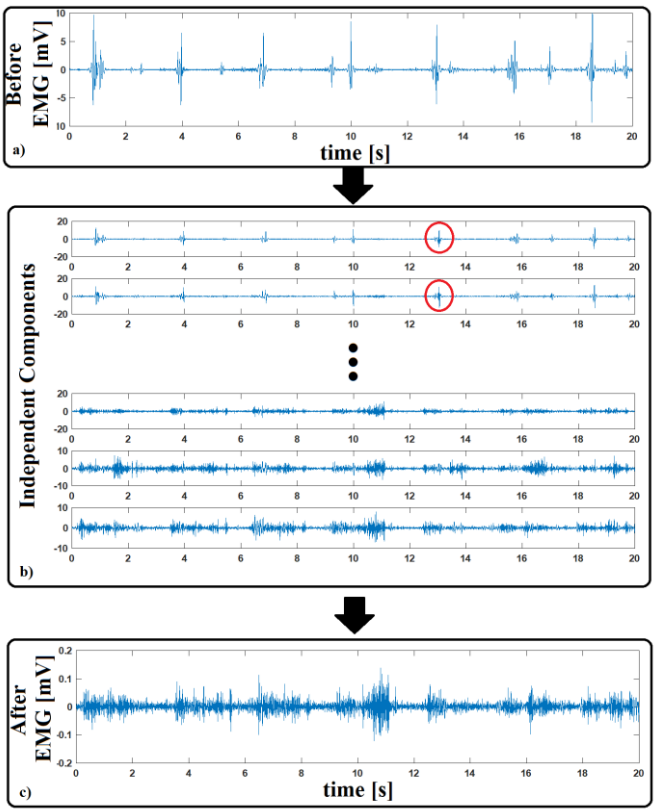

Fig. 2. Removing heel contact artefacts from EMG signals by applying ICA method. a) The example of EMG signal with significant moving electrode artefacts incurred during a heel strike; b) The independent components obtained from 24 EMG channels from the same array electrode; c) The EMG signal with removed artefacts.

We applied low pass Butterworth filter (3rd order, cutoff frequency at 3 Hz) on absolute value of EMG signals to estimate the EMG envelopes. All envelopes were normalized relative to maximal value of all channels in the analyzed sequence.

We used EMG envelopes to obtain the EMG maps. Similar to method we used in our previous researches [13], we applied bicubic ("spline") interpolation to current envelope samples from the same array electrode. The only difference was in initial matrix, due to different shape of array electrode. The EMG maps were formed based on the template matrix (72x101 pixels – one pixel corresponds to 1x1mm of array electrode) that contains three groups of pixels (Fig. 3): 24 original pixels with the envelope samples, placed in appropriate place due to pads order; pixels interpolants; and empty pixels that exceed the array electrode.

Algorithm took the samples of EMG envelopes from same array electrode in the same moment (1 sample per channel – 24 samples in total) and arranged them in appropriate pixels in the template. In next step, algorithm applied interpolation and assigned the scale of colors (deep blue is region without activity and deep red is region with highest activity). Assigning colors is used just for visualization of EMG maps, but it is not a part of further calculations.

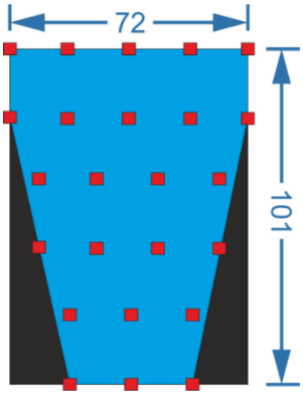

Fig. 3. Template for EMG map interpolation: red squares represent the 24 original data set; blue region represents the pixels interpolants and black region are the empty pixels that exceed dimensions of array electrode.

To ensure better repeatability of EMG maps from step to step, EMG maps were calculated by averaging of 11 samples from each channel, in the vicinity of HC (5 samples before, HC moment and 5 samples after). The number of samples is determined heuristically. Since it is difficult to estimate the appropriate moment from EMG envelopes on the paretic foot, the detection was performed based on signals from the insoles, in which the desired HC is clearly distinguished.

We calculated entropy of digital image as:

$$Ent = -\sum_{i=0}^{n-1} p_i \log p_i \tag{4}$$

where n is number of intensities in the color scale, and p_i is the probability expressed in number of pixels with intensity i. Based on the individual entropies, the mean entropy values for the nonparetic and paretic leg were calculated. A coefficient representing their ratio was calculated, according to the formula:

$$\frac{\overline{Ent_l} - \overline{Ent_r}}{\overline{Ent_l} + \overline{Ent_r}} \tag{5}$$

where $\overline{Ent_l}$ and $\overline{Ent_r}$ are mean entropy values for EMG maps from left and right leg, respectively.

III. Main Results

Figure 4 shows the example of signals from pressure sensors and median of EMG envelopes from nonparetic and paretic leg for seven full gait cycles. Figure also shows sequences of EMG maps on both sides in characteristic moment of gait which are marked with red dots.

In Figure 5 are shown the examples of EMG maps from nonparetic (top left) and paretic (bottom left) leg and their histograms (right).

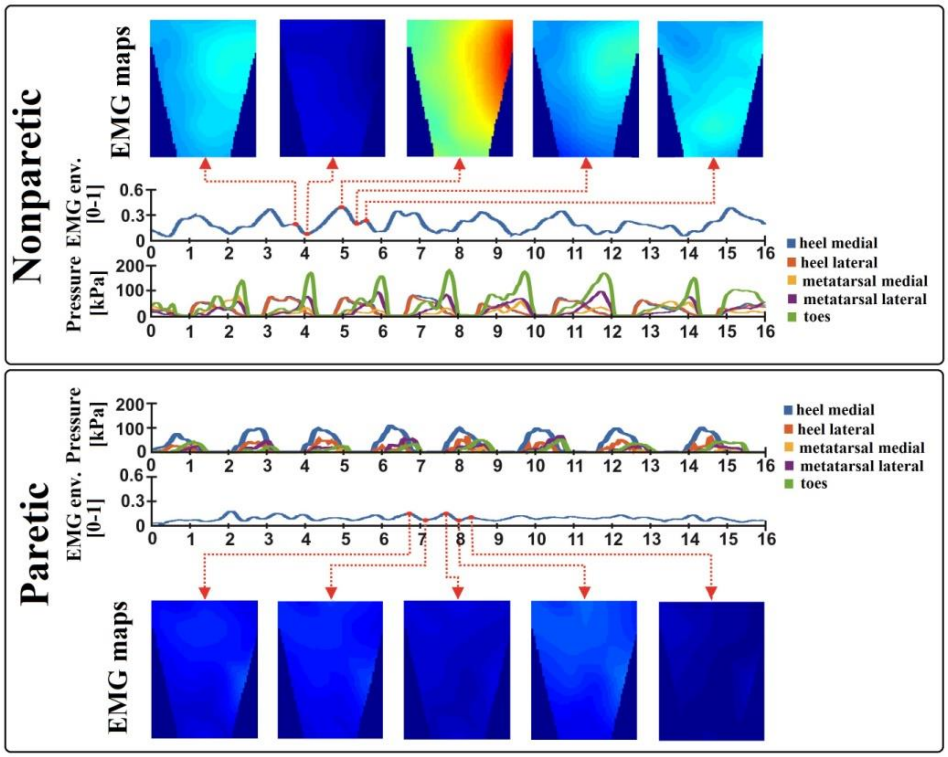

Fig. 4. Signals from pressure sensors and median of EMG envelopes from nonparetic leg (top panel) and paretic leg (bottom panel) for seven full gait cycles; Example shows the sequences of EMG maps on both legs obtained in characteristic moments, marked with red dots. Significant difference can be noticed in signals and EMG maps on paretic and nonparetic side.

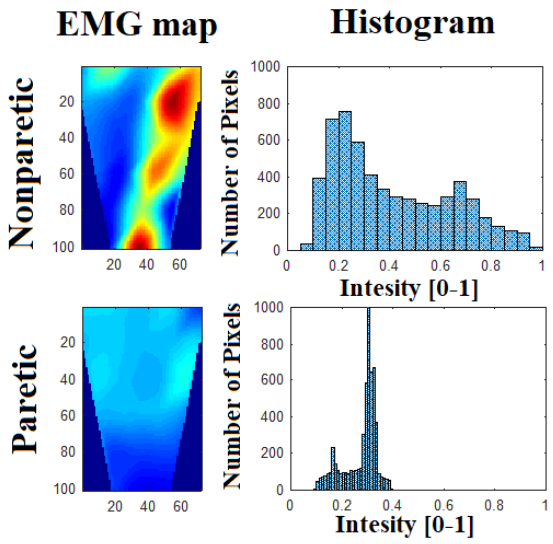

Fig. 5. Examples of EMG maps from nonparetic (top left) and paretic (bottom left) leg and their histograms (right). There is noticeable difference between histograms: histogram on paretic side is more concentrated around one peak, while histogram on nonparetic side wights to uniform distribution.

In Table I are presented the mean values of gait parameters and EMG map entropies obtained from signals recorded before and after therapy. Gait cycle (GC) and Step Cycle (SC) are given in seconds, Swing phase (SWP) and Stance phase (STP) are given as percent of Gait cycle, Gait cadence (GCD) is given in steps per second, Double support phase (DSP) is presented as percent of a Gait cycle and EMG entropy is represented in arbitrary values.

TABLE I
GAIT PARAMETERS AND EMG MAP ENTROPY

		GC [s]	SC [s]	SWP [%]	STP [%]	DSP [%]	GCD [step/s]	Entropy [arb.]
Bef.	L	2.30	0.62	10.3	89.7	50.4	56.27	5.12
	R	2.29	0.61	26.9	73.1	15.7		3.46
Aft.	L	1.86	0.58	17.5	82.5	38.7	70.51	5.43
	R	1.80	0.56	29.8	70.2	17.2		4.07

Figure 6 shows the main ratio between swing and stance phase for paretic and nonparetic leg before and after therapy (left panel) and ratio of EMG entropies on left and right leg before and after therapy (right panel).

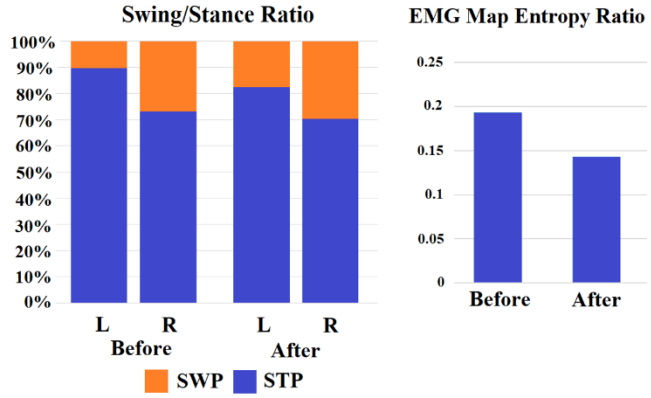

Fig. 6. Main ratio between SWP and STP for paretic and nonparetic leg before and after therapy (left panel) and ratio of EMG map entropies between left and right leg before and after therapy.

IV. Discussion

In Figure 4 it is noticeable that the pressure distribution during the STP arises in an irregular rhythm on the paretic leg (all signals rise simultaneously from the HC moment). Segments in which the pressures are equal to 0 represent the SWP and it can be noticed that their duration differs on the paretic and nonparetic leg: the SWP is shorter on the nonparetic leg, because the subject tends to rely on the nonparetic leg as soon as possible. These differences in signals on both sides indicates to irregular and asymmetrical gait.

In Figure 4 significant difference in EMG activity between nonparetic and paretic leg can be noticed: mean envelope on nonparetic side has relatively repetitive pattern with local maxima at HC moment, while on paretic side EMG envelopes have irregular pattern and noticeably lover amplitude. This difference reflects to EMG maps (Figure 4 top and bottom). Beside lower intensity, EMG maps on paretic side don't have clearly defined high intensity regions, and activity spreads all over the EMG map. This can be explained as patients attempt to make a movement by compensatory mechanism, due to poor innervation of targeted muscle. The EMG maps and histograms in Figure 5 illustrate this scattering of EMG activity. Histogram of nonparetic EMG map wights to uniform distribution because the pixels of the EMG map have various intensities. On the other hand, histogram of the EMG map from paretic side is concentrated around one peak, because the majority of the pixels have same intensity (color).

These differences in intensity distribution are clearly quantified by calculating entropies. The values shown in Table I: 5.12 for nonparetic and 3.46 for paretic leg before the therapy. The greater entropy is the histogram is closer to uniform distribution, which means more different colors in EMG map. After the therapy, difference between entropies are lower, which indicates patient's improvement and greater selectivity in muscle recruitment. The EMG map entropy ratio shown in Figure 6 represents the symmetry of patient's activities on paretic and nonparetic leg and level of selectivity for muscle recruitment. Due to equation (5), in ideal case this ratio would be 0 which would mean that both legs have the same selectivity (entropies are equal on both legs).

Global improvement can be noticed in gait parameters in Table I: patient walks faster (GCD is greater and GC and SC are shorter), but also symmetry is improved (difference between duration of SWP and STP on paretic and nonparetic leg are lower; Figure 6 left panel).

V. Conclusion

The proposed method, which combines the use of pressure sensors with EMG array electrodes and portable amplifiers, provides a good base for gait analysis. The formed set of parameters, based on gait mechanics, and spatio-temporal images of muscle activity during gait (both as a visual assessment and quantified), gives the possibility to assess the patient's condition before and after therapy.

Acknowledgment

This research was supported by the grants III4008 and TR35003 from the Ministry of Education, Science and Technological development of Serbia. The experimental protocol was approved by ethical committee of the Clinic for rehabilitation "Dr Miroslav Zotović" in Belgrade, Serbia.

VI. References

[1] D. B. Popović and T. Sinkjær, Control of movements in humans: systems and mechanisms, Belgrade: Academic Mind, 2015.

[2] C. Ridao-Fernández, E. Pinero-Pinto and G. Chamorro-Moriana, "Observational gait assessment scales in patients with walking disorders: systematic review," *BioMed research international, vol.* 2019, pp. 12, 2019.

[3] K. Aminian, C. Trevisan, B. Najafi, H. Dejnabadi, C. Frigo, E. Pavan, A. Telono, F. Cerati, E. C. Marinoni, P. Robert and P. F. Leyvraz, "Evaluation of an ambulatory system for gait analysis in hip osteoarthritis and after total hip replacement," *Gait & posture,* vol. 20, no. 1, pp. 102-107, 2004.

[4] S. J. M. Bamberg, A. Y. Benbasat, D. M. Scarborough, D. E. Krebs and J. A. Paradiso, "Gait analysis using a shoe-integrated wireless sensor system," *IEEE transactions on information technology in biomedicine*, vol. 12, no. 4, pp. 413-423, 2008.

[5] B. Bilney, M. Morris and K. Webster, ""Concurrent related validity of the GAITRite® walkway system for quantification of the spatial and temporal parameters of gait," *Gait & posture,* vol. 17, no. 1, pp. 68-74, 2003.

[6] I. Milovanović and D. B. Popović, "Principal component analysis of gait kinematics data in acute and chronic stroke patients," *Computational and mathematical methods in medicine,vol. 2012, pp. 8,* 2012.

[7] A. Strazza, A. Mengarelli, S. Fioretti, L. Burattini, V. Agostini, M. Knaflitz and F. Di Nardo, "Surface-EMG analysis for the quantification of thigh muscle dynamic co-contractions during normal gait," *Gait & Posture,* vol. 51, pp. 228-233, 2017.

[8] I. Topalović and D. B. Popović, "Estimation of gait parameters based on data from inertial measurement units," in *Procceedings of 4th IcETRAN*, Kladovo, Serbia, 05-08. June, 2017.

[9] J. Milovanović, M. Gavrilović, I. Topalović and D. B. Popović, "Influence of two weeks balance practice with feedback on the gait in hemiplegic patients," in *IcETRAN & ETRAN*, Palić, Serbia, 11-14. June, 2018.

[10] D. B. Popović, I. Topalović, S. Dedijer Dujović and L. Konstantinović, "Wearable system for the gait assessment in stroke patients," in *International Conference on NeuroRehabilitation. Springer, Cham*, 2018.

[11] L. Popović Maneski, I. Topalović, N. Jovičić, S. Dedijer, L. Konstantinović and D. B. Popović, "Stimulation map for control of functional grasp based on multi-channel EMG recordings," *Medical engineering & physics,* vol. 38, no. 11, pp. 1251-1259, 2016.

[12] L. Popović-Maneski and I. Topalović, "EMG Map for Designing the Electrode Shape for Functional Electrical Therapy of Upper Extremities," in *Masia, L., Micera, S., Akay, M., Pons, J.L. (Eds.),Converging Clinical and Engineering Research on Neurorehabilitation III, Biosystems & Biorobotics*, Pisa, Italy, Springer International Publishing, 2019, pp. 1003-1007.

[13] I. Topalović, S. Graovac and D. B. Popović, "EMG map image processing for recognition of fingers movement," *Journal of Electromyography and Kinesiology,* vol. 49, p. 102364, 2019.

[14] I. Topalović, M. Janković and D. B. Popović, "Validation of the acqusition system Smarting for EMG recordings with electrode arry," in *Proceedings of 2nd Ic ETRAN*, Srebrno Jezero, 08-11. June, 2015.

[15] A. Hyvärinen, "Fast and Robust Fixed-Point Algorithms for Independent Component Analysis," *IEEE Transactions on Neural Networks,* vol. 10, no. 3, pp. 626-634, 1999.